Quark Gluon Plasma and Color Glass Condensate at RHIC? The perspective from the BRAHMS experiment.

VERSION: 9/1/04

I. Arsene[10], I. G. Bearden[7], D. Beavis[1], C. Besliu[10], B. Budick[6], H. Bøggild[7], C. Chasman[1], C. H. Christensen[7], P. Christiansen[7], R. Debbe[1], E. Enger[12], J. J. Gaardhøje[7], M. Germinario[7], K. Hagel[8], O. Hansen[7], A. Holm[7], H. Ito[1,11], A. Jipa[10], F. Jundt[2], J. I. Jørdre[9], C. E. Jørgensen[7], R. Karabowicz[4], E. J. Kim[1], T. Kozik[4], T. M. Larsen[12], J. H. Lee[1], Y. K. Lee[5], S. Lindal[12], R. Lystad[9], G. Løvhøiden[12], Z. Majka[4], A. Makeev[8], M. Mikelsen[12], M. Murray[8,11], J. Natowitz[8], B. Neumann[11], B. S. Nielsen[7], J. Norris[11], D. Ouerdane[7], R. Płaneta[4], F. Rami[2], C. Ristea[10], O. Ristea[10], D. Röhrich[9], B. H. Samset[12], D. Sandberg[7], S. J. Sanders[11], R. A. Scheetz[1], P. Staszel[7,4], T. S. Tveter[12], F. Videbæk[1], R. Wada[8], Z. Yin[9], and I. S. Zgura[10]

[1] Brookhaven National Laboratory, Upton, New York 11973, USA
[2] Institut de Recherches Subatomiques et Université Louis Pasteur, Strasbourg, France
[5] Johns Hopkins University, Baltimore 21218, USA
[4] M. Smoluchkowski Inst. of Physics, Jagiellonian University, Krakow, Poland
[6] New York University, New York 10003, USA
[7] Niels Bohr Institute, University of Copenhagen, Copenhagen 2100, Denmark
[8] Texas A&M University, College Station, Texas, 17843, USA
[9] University of Bergen, Department of Physics, Bergen, Norway
[10] University of Bucharest, Romania
[11] University of Kansas, Lawrence, Kansas 66045, USA
[12] University of Oslo, Department of Physics, Oslo, Norway

We review the main results obtained by the BRAHMS collaboration on the properties of hot and high energy density hadronic and partonic matter produced in ultrarelativistic heavy ion collisions at RHIC. A particular focus of this report, is to discuss to what extent the results collected so far by BRAHMS, and by the other three experiments operating at RHIC, can be taken as evidence for the formation of a state of deconfined partonic matter, the so called quark-gluon-plasma (QGP). We also discuss evidence for a possible precursor state to the QGP, i.e. the proposed Color Glass Condensate.

1. Introduction

From the onset of the formulation of the quark model and the first understanding of the nature of the binding and confining potential between quarks about 30 years ago it has been conjectured that a state of matter characterized by a large density of quarks and

gluons (together called partons) might be created for a fleeting moment in violent nuclear collisions [1]. This high energy density state would be characterized by a strongly reduced interaction between its constituents, the partons, such that the partons would exist in a nearly free state. Aptly, this proposed state of matter has been designated the quark gluon plasma (QGP). It is now generally thought that the early universe was initially in a QGP state until its energy density had decreased sufficiently, as a result of the adiabatic expansion of the universe, that it could make the transition to ordinary (confined) matter.

Experimental attempts to create the QGP in the laboratory and measure its properties have been carried out for more than 20 years, by studying collisions of heavy nuclei and analyzing the fragments and produced particles emanating from such collisions. During that period, center of mass energies per pair of colliding nucleons have risen steadily from the $\sqrt{s_{NN}} \approx 1\,\mathrm{GeV}$ domain of the Bevalac at LBNL, to energies of $\sqrt{s_{NN}} = 5\,\mathrm{GeV}$ at the AGS at BNL, and to $\sqrt{s_{NN}} = 17\,\mathrm{GeV}$ at the SPS accelerator at CERN. No decisive proof of QGP formation was found in the experiments at those energies, although a number of signals suggesting the formation of a 'very dense state of matter' were found at the SPS [2,3].

With the Relativistic Heavy Ion Collider, RHIC, at Brookhaven National Laboratory, the total energy in the center of mass in central collisions between gold nuclei 100 AGeV + 100 AGeV is almost 40 TeV, the largest so far achieved in nucleus-nucleus collisions under laboratory conditions. This energy is so large that conversion of a sizeable fraction of the initial kinetic energy into matter production creates many thousands of particles in a limited volume leading to unprecedented large energy densities and thus presumably ideal conditions for the formation of the quark gluon plasma.

RHIC started regular beam operations in the summer of year 2000 with a short commissioning run colliding Au nuclei at $\sqrt{s_{NN}} = 130\,\mathrm{GeV}$. The first full run at the top energy ($\sqrt{s_{NN}} = 200\,\mathrm{GeV}$) took place in the fall/winter of 2001/2002. The third RHIC run during the winter/spring of 2003 focussed on d+Au and p+p reactions. Recently, in 2004, a long high luminosity Au+Au run at $\sqrt{s_{NN}} = 200\,\mathrm{GeV}$ and a short run at $\sqrt{s_{NN}} = 62.4\,\mathrm{GeV}$ have been completed. The collected data from the most recent runs are currently being analyzed and only a few early results are thus available.

The main aim here is to review the available information obtained from the first RHIC experiments with the purpose of determining what the experimental results, accumulated so far, allow us to say about the high energy density matter that is created at RHIC in collisions between heavy atomic nuclei.

We concentrate primarily on results from the BRAHMS detector, one of the four detectors at RHIC, but naturally also refer to results obtained by the other three experiments (STAR, PHENIX and PHOBOS) insofar as they complement or supplement information obtained from BRAHMS. The BRAHMS experiment is a two arm magnetic spectrometer with excellent momentum resolution and hadron identification capabilities. The two spectrometers subtend only a small solid angle (a few msr) each, but they can rotate in the horizontal plane about the collision point to collect data on hadron production over a wide rapidity range (0-4), a unique capability among the RHIC experiments. For details about the BRAHMS detector system we refer the reader to [4,5]. The large number of articles already produced by the four experiments at RHIC may be found on their respective homepages [6]. Recent extensive theoretical reviews and commentaries may be found

in refs. [7–9].

2. What is the QGP and what does it take to see it?

The predicted transition from ordinary nuclear matter, which consists of hadrons inside which quarks and gluons are confined, to the QGP, a state of matter in which quark and gluons are no longer confined to volumes of hadronic dimensions, can in the simplest approach be likened to the transition between two thermodynamic states in a closed volume.

As energy is transferred to the lower energy state a phase transition, akin to a melting or evaporation process, to the higher energy state occurs. For a first order phase transition (PT), the transformation of one state into the other occurs at a specific temperature, termed the critical temperature, and the process is characterized by absorption of latent heat during the phase conversion, leading to a constancy or discontinuity of certain thermodynamic variables as the energy density is increased. In this picture, it is tacitly assumed that the phase transition occurs between states in thermodynamic equilibrium. From such thermodynamical considerations, and from more elaborate models based on the fundamental theory for the strong interaction, Quantum Chromo Dynamics (e.g. lattice QCD calculations), estimates for the critical temperature and the order of the transition can made. Calculations indicate that the critical temperature should be $T_c \approx 150-180\,\mathrm{MeV}$ in the case of a vanishing baryon chemical potential [10]. In general, a decreasing critical temperature with increasing chemical potential is expected. Likewise, at non-zero chemical potential a mixed phase of coexisting hadron gas, HG, and QGP is predicted to exist in a certain temperature interval around the critical temperature. Recently calculational techniques have progressed to the point of allowing an extension of the lattice methods also to finite chemical potential.

The transition from ordinary matter to the QGP is thus primarily a deconfinement transition. However, it is also expected, due to the vanishing interaction between partons in the QGP phase, that hadron masses will be strongly modified and in fact lowered. In the limit of chiral symmetry the expectation value of the quark condensate ($< q\bar{q} >$ vanishes and opposite parity states (chiral partners) are degenerate. As a consequence of the QGP to HG transition, the chiral symmetry is broken and the hadrons acquire definite and nondegenerate masses. According to predictions from lattice QCD chiral symmetry should be restored at sufficiently high temperature ($T >> T_c$).

It is, however, at the onset not at all clear that the transition to the QGP, as it is expected to be recreated in nucleus-nucleus collisions, proceeds between states of thermodynamic equilibrium as sketched above. The reaction, from first contact of the colliding nuclei to freeze-out of the created fireball, occurs on a typical timescale of about $10\,\mathrm{fm/c}$ and is governed by complex reaction dynamics so that non-equilibrium features may be important. Likewise there can be significant rescattering of the strongly interacting components of the system, after its formation, that tends to obscure specific features associated with a phase transition.

Many potential experimental signatures for the existence of the QGP have been proposed. These can be roughly grouped into two classes: 1) *evidence for bulk properties consistent with QGP formation*, e.g. large energy density, entropy growth, plateau behav-

ior of the thermodynamic variables, unusual expansion and lifetime properties of the system, presence of thermodynamic equilibration, fluctuations of particle number or charge balance etc, and 2) *evidence for modifications of specific properties of particles thought to arise from their interactions with a QGP*, e.g. the modification of widths and masses of resonances, modification of particle production probabilities due to color screening (e.g. J/Ψ suppression) and modification of parton properties due to interaction with other partons in a dense medium (e.g. jet quenching), etc.

We may ask the following questions: *1) What is the requirement for calling a state of matter a QGP?*, and *2) What would constitute proof of QGP formation according to that definition?*

As far as the first question is concerned it would seem obvious that the the determining factor is whether the high density state that is created in the nuclear collisions clearly has properties that are determined by its partonic composition, beyond what is known at the nucleon level in elementary nucleon-nucleon collisions (e.g. p+p collisions). It has often been presupposed that the 'plasma' should be in thermodynamical equilibrium. However, this may not be realized within the short time scales available for the evolution of the reaction from first contact to freeze-out, and is perhaps not necessary in the definition of the version of the QGP that may be observable in relativistic heavy ion collisions. Finally, it may be asked whether chiral symmetry restoration is essential. It would seem that even in a situation in which the partons of the system are still (strongly) interacting one may speak of a QGP as long as the constituents are not restricted to individual hadrons. Thus it would seem that *deconfinement* is the foremost property needed to define the QGP state, and the one that needs to be demonstrated by experiment.

Clearly, the observation of all, or at least of a number of the effects listed above, in a mutually consistent fashion, would serve to constitute a strong case for the formation of a QGP. Ideally, the observed effects must not be simultaneously describable within other frameworks, e.g. those based on purely hadronic interactions and not explicitly involving the partonic degrees of freedom. This suggests the requirement that a 'proof', in addition to having consistency with QGP formation, also must contain elements that are *only* describable in terms of QGP formation, phase transition etc.

Finally, if a sufficiently good case exists, we may also ask if there are any specific features that may *falsify* the conclusion. To our knowledge no tests have been proposed that may allow falsification of either a partonic scenario or a hadronic scenario, but it would be important if any such exclusive tests were to be formulated.

In this report we address some of the signatures discussed above, notably the energy density, which can be deduced from the measured particle multiplicities, the thermal and dynamical properties of the matter at freeze-out which may be inferred from the abundances and spectral properties of identified particles and the modifications of spectral properties arising from the interaction of particles with the high energy density medium.

3. Reactions at RHIC: how much energy is released?

The kinetic energy that is removed from the beam and which can be converted into a material state such as the QGP depends on the amount of stopping between the colliding ions.

The stopping can be estimated from the rapidity loss experienced by the baryons in the colliding nuclei. If incoming beam baryons have rapidity, y_b relative to the CM (which has $y = 0$) and average rapidity

$$< y >= \int_0^{y_b} y \frac{dN}{dy} dy / \int_0^{y_b} \frac{dN}{dy} dy \quad (1)$$

after the collision, the average rapidity loss is $\delta y = y_b - < y >$ [11,12]. Here dN/dy denotes the number of net-baryons (number of baryons minus number of antibaryons) per unit of rapidity. Thus, for the case of full stopping: $\delta y \approx y_b$.

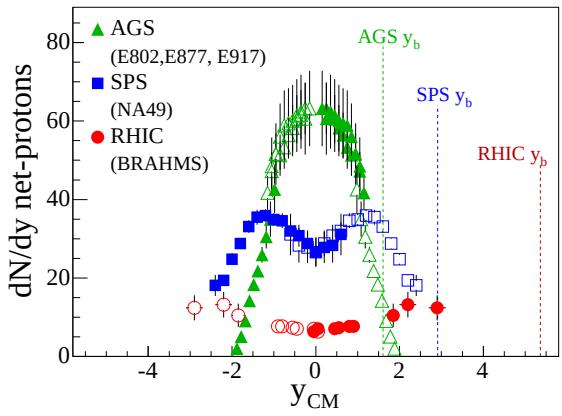

Figure 1. Rapidity densities of net protons (i.e. number of protons minus antiprotons) measured at AGS, SPS, and RHIC(BRAHMS)for central collisions. At RHIC, the full distribution cannot be measured with current experiments, but BRAHMS will be able to extend its results to y=3.5 from the most recent run, corresponding to measurements at 2.3 degrees with respect to the beam.

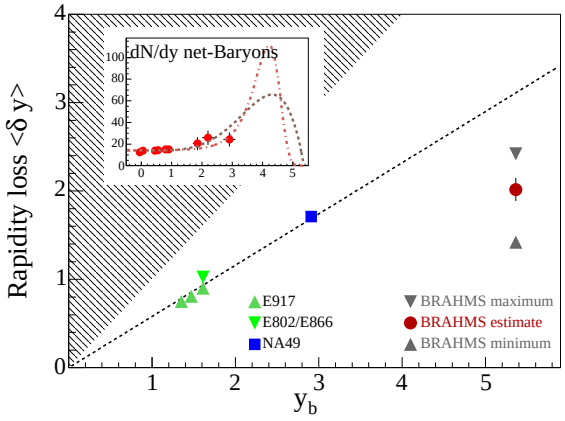

Figure 2. Insert: estimates of possible net-baryon distributions requiring baryon number conservation. We have assumed that $N(n) \approx N(p)$ and scaled hyperon yields at midrapidity to forward rapidity using HIJING. From these extremes, quite tight limits on the rapidity loss of colliding Au ions at RHIC can be set (main panel).

At AGS energies the number of produced antibaryons is quite small and the net-baryon distribution is similar to the proton distribution [14–16]. The net-proton rapidity distribution is centered around $y = 0$ and is rather narrow. The rapidity loss is about 1 for a beam rapidity of approx. 1.6. At CERN-SPS energies ($\sqrt{s_{NN}} = 17\,\mathrm{GeV}, 158\,\mathrm{AGeV}$ Pb+Pb reactions) the rapidity loss is slightly less than 2 for a beam rapidity of 2.9 [17], about the same relative rapidity loss as at the AGS. The fact that the rapidity loss is large on an absolute scale means, however, that there is still a sizeable energy loss of the colliding nuclei. This energy is available for particle production and other excitations. Indeed, in collisions at the SPS, multiplicities of negatively charged hadrons are about $dN/dy = 180$

around $y = 0$. At SPS another feature is visible (see fig. 1): the net proton rapidity distribution shows a double 'hump' with a dip around $y = 0$. This shape results from the finite rapidity loss of the colliding nuclei and the finite width of each of the humps, which reflect the rapidity distributions of the protons after the collisions. This picture suggests that the reaction at the SPS is beginning to be transparent in the sense that fewer of the original baryons are found at midrapidity after the collisions, in contrast to the situation at lower energies.

BRAHMS has measured the net proton rapidity distribution at RHIC in the interval $y = 0-3$ in the first run with $(0-10\%)$ central Au+Au collisions at full energy. The beam rapidity at RHIC is about 5.4. Details of the analysis can be found in [18]. The results are displayed in fig. 1 together with the previously discussed net-proton distributions measured at AGS and SPS. The RHIC distribution is both qualitatively and quantitatively very different from those at lower energies indicating a significantly different system is formed near midrapidity.

The net number of protons per unit of rapidity around $y = 0$ is only about 7 and the distribution is flat over at least the ± 1 unit of rapidity. The distribution increases in the rapidity range $y = 2 - 3$ to an average $dN/dy \approx 12$. We have not yet completed the measurements at the most forward angles (highest rapidity) allowed by the geometrical setup of the experiment, but we can exploit baryon conservation in the reactions to set limits on the relative rapidity loss at RHIC. This is illustrated in fig. 2, which shows two possible distributions whose integral areas correspond to the number of baryons present in the overlap between the colliding nuclei. From such distributions one may deduce a set of upper and lower limits for the rapidity loss at RHIC. Furthermore the situation is complicated by the fact that not all baryons are measured. The limits shown in the figure includes estimates of these effects [18]. The conclusion is that the *absolute* rapidity loss at RHIC ($\delta y = 2.0 \pm 0.4$) is not appreciably larger than at SPS. The value is close to expectations from extrapolations of pA data at lower energies [12,13] In fact the *relative* rapidity loss is significantly reduced as compared to an extrapolation of the low energy systematics [11].

It should be noted that the rapidity loss is still significant and that, since the overall beam energy (rapidity) is larger at RHIC than at SPS, the *absolute energy loss* increases appreciably from SPS to RHIC thus making available a significantly increased amount of energy for particle creation in RHIC reactions.

In particular we have found that the average energy loss of the colliding nuclei corresponds to about $73 \pm 6\,\mathrm{GeV}$ per nucleon[18]. From our measurements of the particle production as a function of rapidity (pions, kaons and protons and their antiparticles) we can deduce not only the number of produced particles but also their average transverse momentum and thus their energy. Within systematic errors of both measurements we find that the particle production is consistent with the energy that is taken from the beam.

Thus the energy loss measurements clearly establish that as much as $26\,\mathrm{TeV}$ *of kinetic energy is removed from the beam per central Au+Au collision. This energy is available for particle production in a small volume immediately after the collision.*

4. Energy density

The collision scenario that we observe at RHIC and which was outlined in the previous section indicates that the reaction can be viewed as quite transparent. After the collision, the matter and energy distribution can be conceptually divided up into two main parts, a so–called fragmentation region consisting of the excited remnants of the colliding nuclei which have experienced an average rapidity loss of about 2.0, and a central region in which few of the original baryons are present but where significant energy density is collected.

This picture is in qualitative agreement with the schematic one already proposed by Bjorken 20 years ago [19]. The central region (an interval around midrapidity) is decoupled from the fragments. In that theoretical scenario the energy removed from the kinetic energy of the fragments is initially stored in a color field strung between the receding partons that have interacted. The linear increase of the color potential with distance eventually leads to the production of quark-antiquark pairs. Such pairs may be produced anywhere between the interacting partons leading to an approximately uniform particle production as a function of rapidity and similar spectra characteristics in each frame of reference (boost invariance).

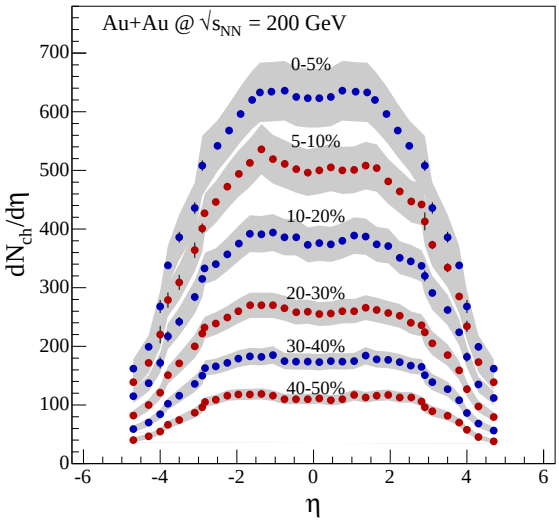

Figure 3. Pseudorapidity densities (multiplicities) of charged particles measured by BRAHMS for $\sqrt{s_{NN}} = 200\,GeV$) Au+Au collisions. The integral of the most central distribution $0-5\%$ corresponds to about 4600 charged particles [5].

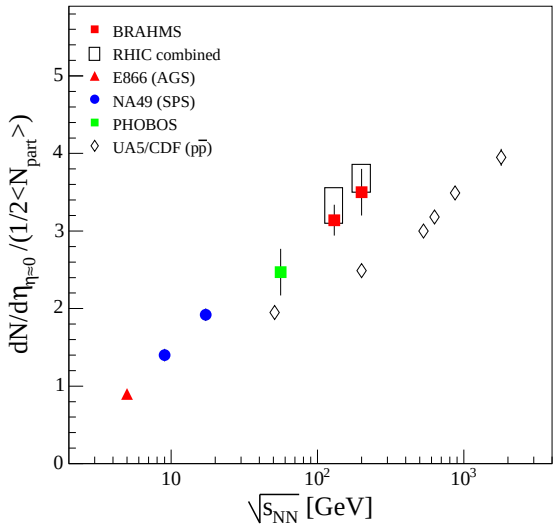

Figure 4. Multiplicity of charged particles per participant pair as a function of $\sqrt{s_{NN}}$. The figure shows that the particle production around midrapidity exceeds that seen in p+p collisions by 40-50%.

Figure 3 shows the overall multiplicity of charged particles observed in Au+Au collisions at RHIC [5] for various collision centralities and as a function of pseudorapidity. The

figure shows that the multiplicity at RHIC is about $dN/d\eta = 625$ charged particles per unit of rapidity around $\eta = 0$ for central collisions. Figure 4 shows that the production of charged particles in central collisions exceeds the particle production seen in p+p collisions at the same energy by 40-50%, when the yield seen in p+p collisions is multiplied by the number of participant pairs of nucleons(participant scaling).

Integration of the charged particle pseudorapidity distributions corresponding to central collisions tells us that about 4600 charged particles are produced in each of the 5% most central collisions. Since we only measure charged particles, and not the neutrals, we multiply this multiplicity by 3/2 to obtain the total particle multiplicity of about 7000 particles.

From the measured spectra of pions, kaons and protons and their antiparticles as a function of transverse momentum we can determine the average transverse mass for each particle species (fig. 5). This allows us to estimate the initial energy density from Bjorkens formula [19]

$$\epsilon = \frac{1}{\pi R^2 \tau} \frac{d\langle E_T \rangle}{dy} \tag{2}$$

where we can make the substitution $d\langle E_T \rangle = \langle m_T \rangle dN$ and use quantities from the measured spectral distributions. Since we wish to calculate the energy density in the very early stages of the collision process we may use for R the radius of the overlap disk between the colliding nuclei, thus neglecting transverse expansion. The formation time is more tricky to determine [20,21]. It is often assumed to be of the order of 1 fm/c, a value that may be inferred from the uncertainty relation and the typical relevant energy scale (200 MeV). Under these assumptions we find that $\epsilon \approx 5\,\mathrm{GeV/fm^3}$, which should be considered as a lower limit. This value of the initial energy exceeds the energy density of a nucleus by a factor of 30 the energy density of a baryon by a factor of 10, and the energy density for QGP formation that is predicted by lattice QCD calculations by a factor of 5 [22,23].

The particle multiplicities that are observed at RHIC indicate that the energy density associated with particle production in the initial stages of the collisions largely exceeds the energy density of hadrons.

5. Is there thermodynamical and chemical equilibrium at RHIC?

It has traditionally been considered crucial to determine whether there is thermodynamical equilibration of the 'fireball' in relativistic collisions. The main reason is that, if there is thermalization, the simple two phase model may be invoked and the system should evidence the recognizable features of a phase transition.

In nuclear collisions, however, the time scale available for equilibration is very short and the entire system only lives in the order of 10 fm/c. Consequently, it is not evident that the system will evolve through equilibrated states. If equilibrium is established, it would suggest that the system existed for a short time in a state with sufficiently short mean free path. A central issue is whether equilibrium is established in the hadronic cloud in the later stages of the collisions just prior to freeze-out or whether it is established on the partonic level prior to hadronization [24]. Thus, even if equilibration *per se* is probably not a requirement for defining the QGP, it may prove to be an important tool in *identifying* the QGP.

5.1. Particle yields

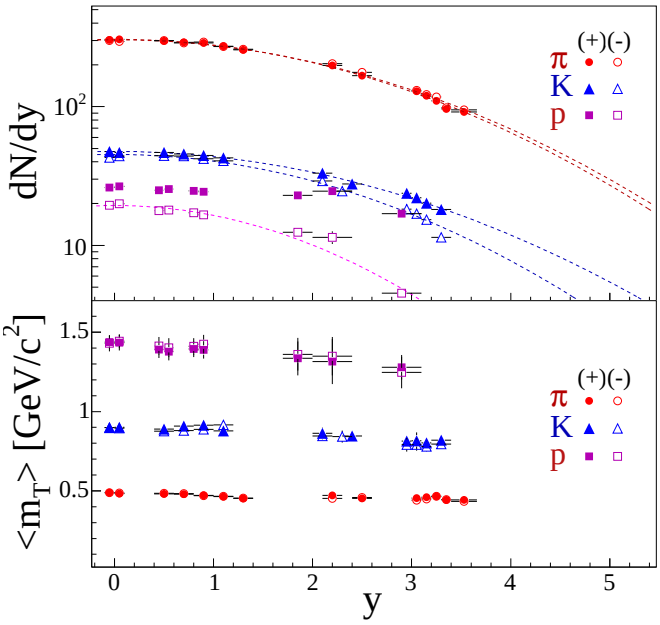

Figure 5. Top: rapidity density distribution for positive and negative pions, kaons and protons. The lines show Gaussian fits. Middle: average m_T distributions as a function of rapidity.

Figure 5 shows a recent and more detailed study of the particle production in central collisions as a function of rapidity [18,25]. The figure shows the rapidity densities of pions and kaons for central collisions. From such distributions we can construct the ratio of the yields of particles and their antiparticles as a function of rapidity. Figure 6 shows the ratios of yields of antihadrons to hadrons (posititive pions, kaons and protons and their antiparticles). The ratio is seen to be approaching unity in an interval of about 1.5 units of rapidity around midrapidity, suggesting that the particle production in the central region is predominantly from pair creation. This is true for pions (ratio of 1), but less so for kaons (ratio=0.95) and protons (ratio= 0.76). There are processes that break the symmetry between particles and antiparticles that depend on the net-baryon distribution discussed in the previous section. One such process that is relevant for kaons is the associated production mechanism (e.g. $p + p \rightarrow p + \Lambda + K^+$) which leads to an enrichment of positive kaons in regions where there is an excess of baryons. Support for this view is given by fig. 7, which shows the systematics of kaon production relative to pion production as a function of center of mass energy. At AGS, where the net proton density is high at midrapidity, the rapidity density of K^+ strongly exceeds that of K^-. In contrast, at RHIC, production of K^+ and K^- is almost equal. This situation changes, however, at larger rapidities where the net proton density increases.

From the measured yields of identified particles as a function of rapidity and their

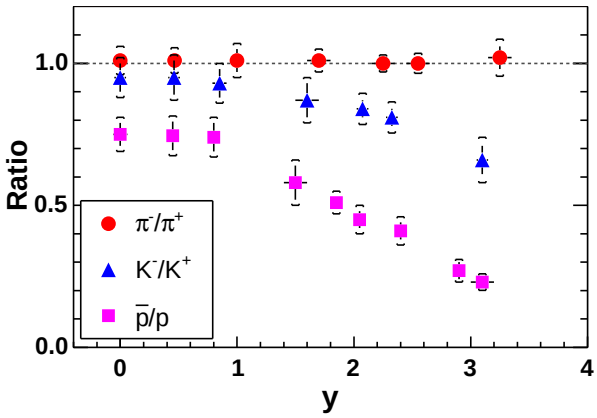

Figure 6. Ratios of antiparticles to particles (pions, kaons and protons) as a function of rapidity for $\sqrt{s_{NN}} = 200\,\mathrm{GeV}$ Au+Au collisions measured by the BRAHMS experiment [26]. For the first time in nuclear collisions an approximate balance between particles and antiparticles is seen around midapidity.

momentum spectra we may calculate the total relativistic energy carried by produced particles in the rapidity interval $y = 0 - 3$. This is shown in fig. 8. By integrating and reflecting the total energy distribution around $y = 0$ and adding the estimate contribution from neutrals we may deduce that about 9 TeV are carried by the produced particles in the rapidity range $|y| < 3$.

The particle yields measured by BRAHMS also lend themselves to an analysis of the charged particle production in terms of the statistical model [26–32]. Figure 9 shows the ratios of negative kaons to positive kaons as a function of the corresponding ratios of antiprotons to protons for various rapidities at RHIC. The data are for central collisions, and the figure also displays similar ratios for heavy ion collisions at AGS and SPS energies. There is a striking correlation between the RHIC/BRAHMS kaon and proton ratios over 3 units of rapidity. Assuming that we can use statistical arguments based on chemical and thermal equilibrium at the quark level, the ratios can be written

$$\frac{\rho(\bar{p})}{\rho(p)} = exp(\frac{-6\mu_{u,d}}{T}) \tag{3}$$

and

$$\frac{\rho(K^-)}{\rho(K^+)} = exp(\frac{-2(\mu_{u,d} - \mu_s)}{T}) = exp(\frac{2\mu_s}{T}) \times [\frac{\rho(\bar{p})}{\rho(p)}]^{\frac{1}{3}} \tag{4}$$

where ρ, μ and T denote number density, chemical potential and temperature, respectively. From equation 3 we find the chemical potential for u and d quarks to be around 25 MeV, the lowest value yet seen in nucleus-nucleus collisions. Equation 4 tells us that for a vanishing strange quark chemical potential we would expect a power law relation between the two ratios with exponent 1/3. The observed correlation deviates from the naive expectation suggesting a finite value of the strange quark chemical potential.

A more elaborate analysis assuming a grand canonical ensemble with charge, baryon and strangeness conservation can be carried out by fitting these and many other particle

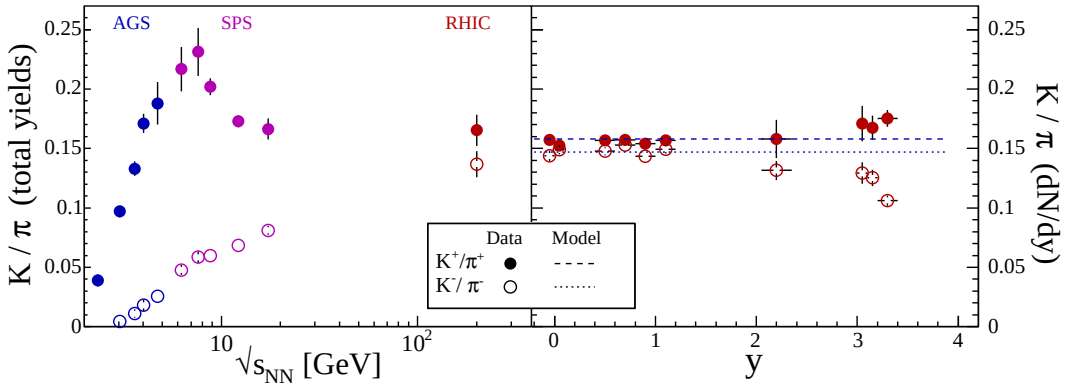

Figure 7. Ratios of kaons and pions of both charge signs as a function of center of mass energy in the nucleon-nucleon system at midrapidity. At top RHIC energy the two ratios are about the same and equal to 0.15 [25]. The lines show predictions, assuming a temperature of 177 MeV and $\mu_B = 29$ MeV.

ratios observed at RHIC in order to obtain the chemical potentials and the temperature. It is found that a very large collection of such particle ratios are extremely well described by the statistical approach [30,32]. An example of such a procedure is shown in fig. 9 and displayed with the full line [31]. Here the temperature is 170 MeV. The point to be made is that the calculation agrees with the data over a wide energy range (from SPS to RHIC) and over a wide range of rapidity at RHIC. This may be an indication that the system is in chemical equilibrium over the considered $\sqrt{s}$ and y ranges (or at least locally in the various y bins). However, that statistical fits reproduce particle ratios is a only a necessary condition for equilibration. Separate measurements at RHIC of, for example, elliptical flow also suggest that the system behaves collectively and thus that the observed ratios are not just due to the filling of phase space according to the principle of maximum entropy.

5.2. Flow

The properties of the expanding matter in the later stages of the collisions up to the moment when interactions cease (kinetic freeze out) can be studied from the momentum distribution of the emitted particles. The slopes of spectra of emitted particles depend in general on the temperature of the source from which they were created and on kinetic effects that may alter the expected Maxwellian distribution, such as a velocity component resulting from an overpressure leading to an outwards flow of the matter. This flow is expected, in the case of (at least local) thermal equilibrium and sufficient density, to be describable by concepts derived from fluid dynamics. It is to be noted that the slopes of spectra reflect the particle distributions at the time when interactions have ceased and thus the obtained physical quantities should be associated with the conditions at freeze-out.

In the so-called blastwave approach the spectrum shape is parametrized by a function

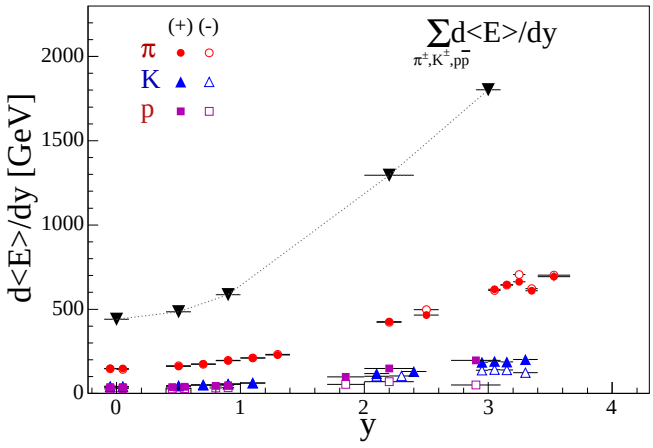

Figure 8. Total relativistic energy of charged hadrons as a function of rapidity.

depending on the temperature and on the transverse expansion velocity which in turn depends on the radius. The result of such analyses for several particle/antiparticle species indicates that the thermal (freezeout) temperature is in the range $T = 120 - 140$ MeV and that the maximum flow velocity is about $0.70c - 0.75c$ as displayed in fig. 10. The first quantity is found, as expected, to be lower than the temperature of the chemical freeze out discussed in the previous subsection. Indeed, it would be expected that the freeze-out of particle ratios occurs earlier than the kinetic freeze out of the particles. The flow velocity component is larger than what was observed at SPS energies. This is consistent with a large pressure gradient in the transverse direction resulting from a large initial density. Fig.10 shows results from analysis of midrapidity particle spectra from the BRAHMS experiment using the blastwave approach.

Another powerful tool to study the thermodynamic properties of the source is the analysis of the azimuthal momentum distribution of the emitted particles relative to the event plane (defined as the direction of the impact parameter). This distribution is usually parametrized as a series of terms depending on $cos(n(\phi - \phi_r))$, where ϕ and ϕ_r denote the azimuthal angles of the particle and of the reaction plane, respectively. The coefficient (v_1) to the n=1 term measures the so-called directed flow and the coefficient (v_2) to the n=2 term measures the elliptic flow. Elliptic flow has been analyzed at RHIC [33–38] and has been found to reach (for many hadron species) large (v_2) values consistent with the hydrodynamical limit and thus of equilibration. Model calculations suggest [39–45] that the observed persistence of azimuthal momentum anisotropy indicates that the system has reached local equilibrium very quickly and that the equilibrium can only be established at the *partonic* level when the system is very dense and has many degrees of freedom. This explanation presupposes however that there are many interactions and thus that the dense partonic phase is strongly interacting.

The particle ratios observed at RHIC can be well described by concepts from statistical physics applied at the quark level, thus assuming thermodynamical equilibrium. However this is only a necessary condition and not a sufficient condition for equilibration. The observation of a strong elliptic flow at RHIC and comparison to model calculation suggests

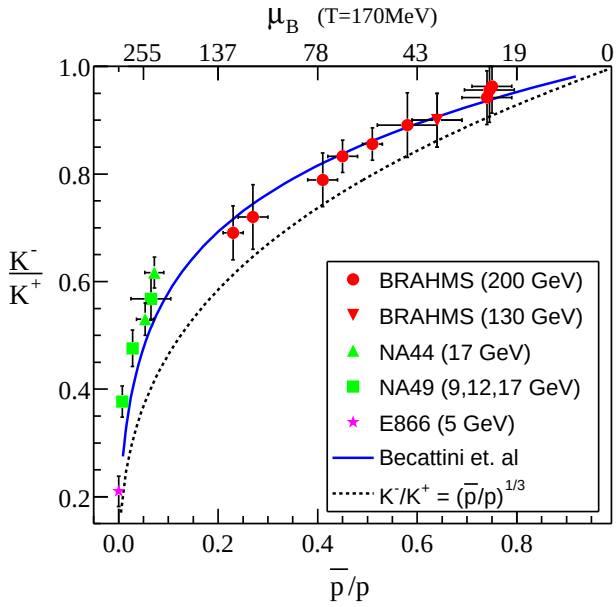

Figure 9. Correlation between the ratio of charged kaons and the ratio of antiprotons to protons. The dashed curve corresponds to equation 3 in the text. The full drawn curve is a statistical model calculation with a chemical freeze-out temperature of 170 MeV [26,31].

that the system is strongly collective as must be the case for an equilibrated system.

6. High p_T suppression. The smoking gun of QGP?

The discussion in the previous sections indicates that the conditions for particle production in a interval $|y| \lesssim 1.5$ at RHIC are radically different than for reactions at lower energies. At RHIC the central zone is baryon poor, the considered rapidity interval appears to approximately exhibit the anticipated boost invariant properties, the particle production is large and dominated by pair production and the energy density appears to exceed significantly the one required for QGP formation. The overall scenario is therefore consistent with particle production from the color field, formation of a QGP and subsequent hadronization. Correlation and flow studies suggest that the lifetime of the system is short ($< 10 fm/c$) and, for the first time, there is evidence suggesting thermodynamic equilibrium already at the partonic level.

But, is this interpretation unique? And, can more mundane explanations based on a purely hadronic scenario be excluded? In spite of the obvious difficulties in reconciling the high initial energy density with hadronic volumes, a comprehensive answer to this question requires the observation of an effect that is directly dependent on the partonic or hadronic nature of the formed high density zone.

6.1. High p_T suppression at midrapidity: final state partonic energy loss?

Such an effect has recently been discovered at RHIC and is related to the suppression of the high transverse momentum component of hadron spectra in central Au+Au collisions as compared to scaled momentum spectra from p+p collisions [46–49]. The effect, originally proposed by Bjorken, Gyulassy and others [50–53] is based on the expecta-

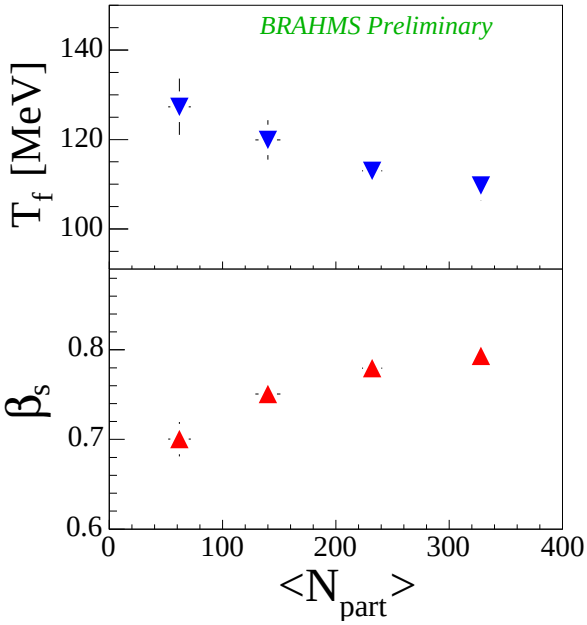

Figure 10. Temperature and transverse flow velocity as a function of collision centrality for Au+Au collisions at midrapidity. BRAHMS preliminary.

tion of a large energy loss of high momentum partons, scattered in the initial stages of the collisions, in a medium with a high density of free color charges [54]. According to QCD colored objects may lose energy by radiating gluons as bremsstrahlung. Due to the color charge of the gluons, the energy loss is proportional to the square of the length of color medium traversed. Such a mechanism would strongly degrade the energy of leading partons resulting in a reduced transverse momentum of leading particles in the jets that emerge after fragmentation into hadrons. The STAR experiment has shown that the topology of high-$p_T$hadron emission is consistent with jet emission, so that we may really speak about jet-suppression [55].

The two upper rows of fig. 11 show our measurements [46,56] of the so-called nuclear modification factors for *unidentified* charged hadrons from Au+Au collisions at rapidities $\eta = 0$ and 2.2. The nuclear modification factor is defined as:

$$R_{AA} = \frac{d^2N^{AA}/dp_t d\eta}{< N_{bin} > d^2N^{NN}/dp_t d\eta}. \tag{5}$$

It involves a scaling of measured nucleon-nucleon transverse momentum distributions by the number of expected incoherent binary collisions, N_{bin}. In the absence of any modification resulting from the 'embedding' of elementary collisions in a nuclear collision we expect $R_{AA} = 1$ a high-p_T. At low p_T, where the particle production follows a scaling with the number of participants, the above definition of R_{AA} leads to $R_{AA} < 1$ for $p_T < 2\,\mathrm{GeV/c}$.

In fact, it is found that $R_{AA} > 1$ for $p_T > 2\,\mathrm{GeV/c}$ in nuclear reactions at lower energy. This enhancement, first observed by Cronin, is associated with multiple scattering of

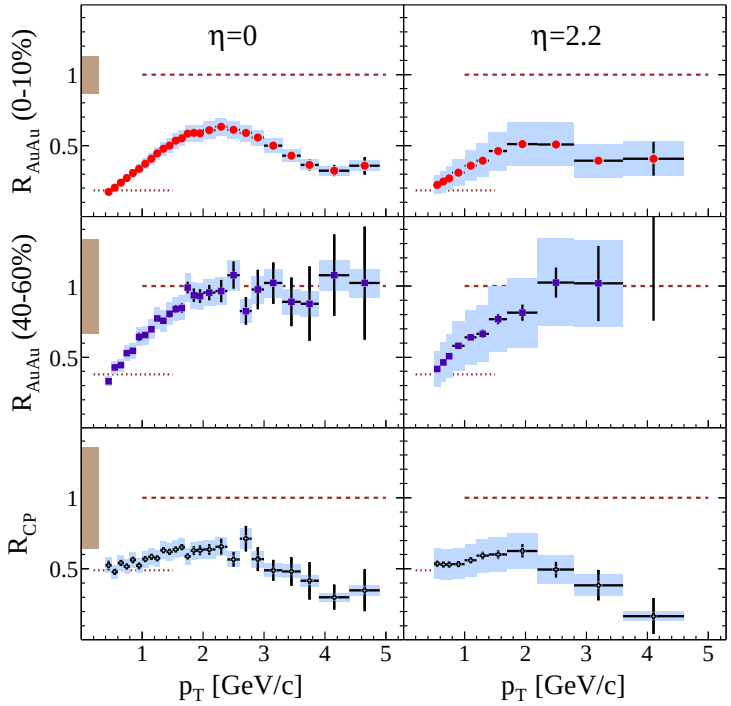

Figure 11. Nuclear modification factors R_{AuAu} as defined in the text, for central and semi-peripheral Au+Au collisions at midrapidity (left) and forward rapidity (right). The lower row shows the factor R_{cp}, i.e. the ratio of the R_{AuAu} for central and peripheral collisions, which has the property of being independent of the p+p reference spectrum [46].

partons [57,58].

Figure 11 demonstrates that, surprisingly, $R_{AA} < 1$ also at high p_T for central collisions at both pseudorapidities, while $R_{AA} \approx 1$ for more peripheral collisions. It is remarkable that the suppression observed at $p_T \approx 4\,\mathrm{GeV/c}$ is very large, amounting to a factor of 3 for central Au+Au collisions as compared to $p + p$ and a factor of more than 4 as compared to the more peripheral collisions. Such large suppression factors are observed at both pseudorapidities.

The very large suppression observed in central Au+Au collisions must be quantitatively understood and requires systematic dynamic modelling. At $\eta = 0$ the particles are emitted at 90 degrees relative to the beam direction, while at $\eta = 2.2$ the angle is only about 12 degrees. In a naive geometrical picture of an absorbing medium with cylindrical symmetry around the beam direction, the large suppression seen at forward angles suggests that the suppressing medium is extended also in the longitudinal direction. Since the observed high-$p_T$suppression is similar or even larger at forward rapidity as compared to midrapidity (see fig. 12) one might be tempted to infer a longitudinal extent of the dense medium which is approximately similar to its transverse dimensions. However, the problem is more complicated, due to the significant transverse and in particular longitudinal expansion that occurs as the leading parton propagates through the medium, effectively reducing the densities of color charges seen. Also other high-$p_T$suppressing mechanisms may come

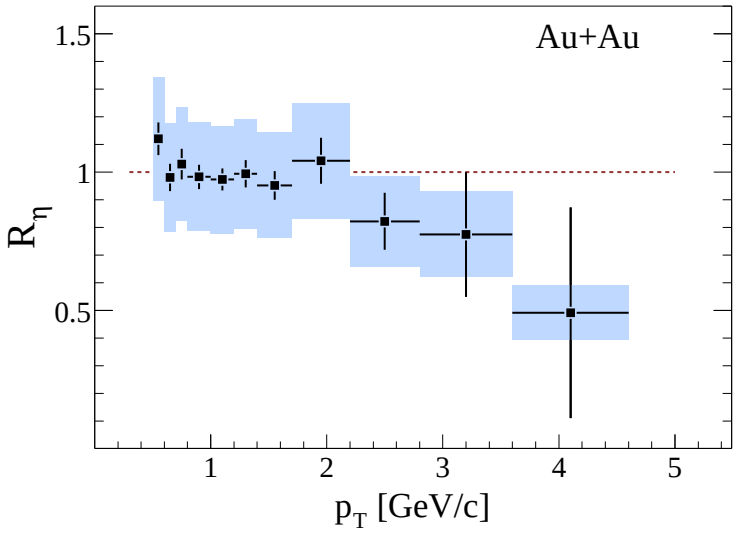

Figure 12. Ratio, R_η, of the suppression factors R_{cp} at pseudorapidities $\eta = 0$ and $\eta = 2.2$ shown in figure 11. The figure suggest that high p_T suppression persists (and is even more important) at forward rapidity than at $\eta = 0$ [46].

into play at forward rapidities (see discussion on the Color Glass Condensate in the following chapter).

It has been conjectured that the observed high-$p_T$suppression might be the result of an entrance channel effect, for example due to a limitation of the phase space available for parton collisions related to saturation effects [59] in the gluon distributions inside the swiftly moving colliding nucleons (which have $\gamma = 100$). As a test of these ideas we have determined the nuclear modification factor for 100 AGeV d + 100 AGeV Au minimum bias collisions. The resulting R_{dAu} is shown in fig. 13 where it is also compared to the R_{AuAu} for central collisions previously shown in fig. 11. No high-p_T jet suppression is observed for d+Au [46,60–62]. The R_{dAu} distribution at $y = 0$ shows a Cronin enhancement similar to that observed at lower energies [17,63,64]. At $p_T \approx 4\,\mathrm{GeV/c}$ we find a ratio $R_{dAu}/R_{AuAu} \approx 4 - 5$. These observations are consistent with the smaller transverse dimensions of the overlap disk between the d and the Au nuclei and also appear to rule out initial state effects.

High-p_T suppression at forward rapidities may also be expected due to the possible existence of a Color Glass Condensate phase in the colliding nuclei (see the discussion in the next section). There is little doubt that systematic studies of the high p_T-jet energy loss as a function of the thickness of the absorbing medium obtained by varying the angle of observation of high p_T jets relative to the event plane and the direction of the beams will be required in order to understand in detail the properties of the dense medium.

6.2. The flavor composition

With its excellent particle identification capabilities BRAHMS can also study the dependence of the high-p_T suppression on the type of particle. Preliminary results [56,65] indicate that mesons (pions and kaons) experience high p_T suppression while baryons (protons) do not. The reason for this difference is at present not well understood.

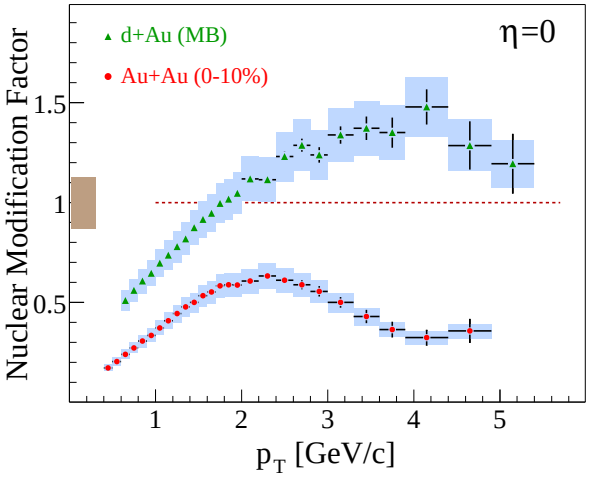

Figure 13. Nuclear modification factors measured for central Au+Au collisions and minimum bias d+Au collisions at $\sqrt{s_{NN}} = 200\,\mathrm{GeV}$, evidencing the important high-$p_T$suppression observed in central Au+Au collisions [46].

The observed difference may be due to the fact that baryons, due to their larger mass, are more sensitive to flow than mesons with the consequence that their transverse momentum spectrum is flatter than for mesons, thus compensating for a possible high p_T suppression similar to that of the mesons. It is also possible that the difference reflects details associated with the the fragmentation mechanism that leads to different degrees of suppression of the high p_T component for 2 and 3 valence quark systems. Finally the difference may reflect the mechanism of recombination for 3 quarks relative to that for 2 quarks in a medium with a high density of quarks.

Figure 14 shows a recent investigation by BRAHMS (ref. [65]) of the baryon to meson ratios at mid-rapidity p/π^+ and $\bar{p}/\pi^-$, as a function of p_T for the 0-10% most central Au+Au collisions at $\sqrt{s_{NN}} = 200$ GeV. The ratios increase rapidly at low p_T and the yields of both protons and anti-protons are comparable to the pion yields for $p_T > 2\,\mathrm{GeV/c}$. The corresponding ratios for $p_T > 2\,\mathrm{GeV/c}$ observed in $p+p$ collisions at $\sqrt{s} = 62$ GeV [66] and in gluon jets produced in $e^+ + e^-$ collisions [67] are also shown. The increase of the p/π^+ and $\bar{p}/\pi^-$ ratios at high p_T, seen in central Au+Au collisions, relative to the level seen in $p+p$ and $e^+ + e^-$ indicates significant differences in the overall description, either at the production or fragmentation level.

Figure 15 shows the comparison of BRAHMS data for the ratio of antiprotons to negative pions at $\eta = 0$ and 2.2. Although statistics at high transverse momentum are low there are indications that the ratio is smaller at the higher rapidity for $p_T > 2GeV$. Recent calculations based on a parton recombination scenario [68–70] with flow at the partonic level appear to be able to describe the data at midrapidity, while calculations omitting flow fall short of the data already at $p_T \approx 1.5\,\mathrm{GeV}$.

The experimental and theoretical investigation of these questions is, however, still in its infancy. These issues can and will be addressed in depth through the analysis of the large data set collected by BRAHMS in the high luminosity Au+Au run of year 2004.

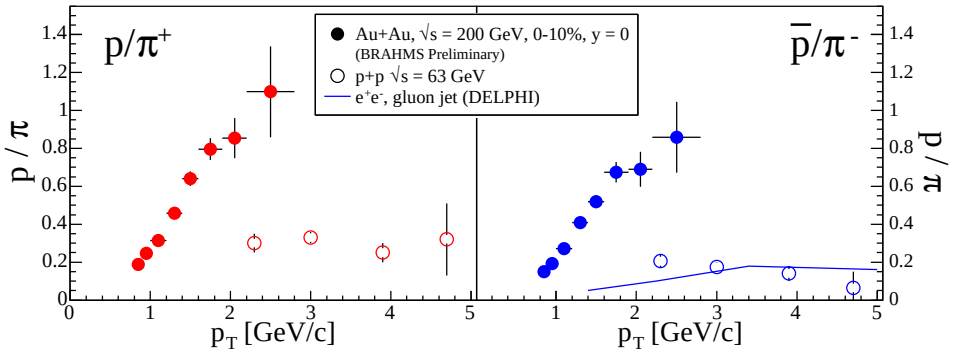

Figure 14. p/π^+ (left) and $\bar{p}/\pi^-$ (right) ratios at mid-rapidity for 0-10% central Au+Au collisions at $\sqrt{s_{NN}} = 200\,\mathrm{GeV}$. The error bars show the statistical errors. The systematic errors are estimated to be less than 8%. Data at $\sqrt{s} = 63\,\mathrm{GeV}$ $p+p$ collisions [66] are also shown. The solid line is the $(p+\bar{p})/(\pi^+ + \pi^-)$ ratio measured in gluon jets [67].

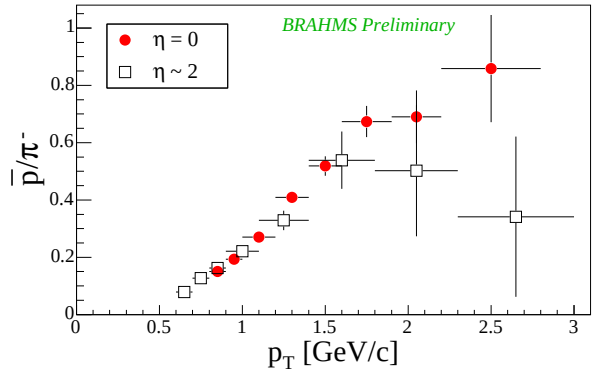

Figure 15. Ratios of $\bar{p}/\pi^-$ at rapidities $y = 0$ and $y = 2.2$. BRAHMS preliminary [65]

6.3. High-p_T suppression at lower energy?

The short commissioning run for Au+Au collisions at $\sqrt{s_{NN}} = 62.4\,\mathrm{GeV}$ has allowed us to carry out a first analysis of the high p_T suppression of charged hadrons at an energy of about 1/3 the maximum RHIC energy and about 3.5 times the maximum SPS energy. Preliminary results are shown in figure 16 for nuclear modification factor calculated for the sum of all charged hadrons measured at 45 degrees($\eta = 1.1$) with respect to the beam direction. The data have been compared to reference spectra measured in $\sqrt{s_{NN}} = 63\,\mathrm{GeV}$ p+p collisions at the CERN-ISR. The figure shows that the degree of high p_T suppression at the lower energy is less important than at $\sqrt{s_{NN}} = 62\,\mathrm{GeV}$. This consistent with recent results from PHOBOS [72]. For comparison, at SPS energies no high p_T suppression was observed, (albeit a discussion has surfaced regarding the accuracy of the reference spectra at that energy). It thus seems the suppression increases smoothly with high energy

The remarkable suppression of high p_T jets at mid-rapidity identified at RHIC is an important signal that evidences the interaction of particles originating from hard parton

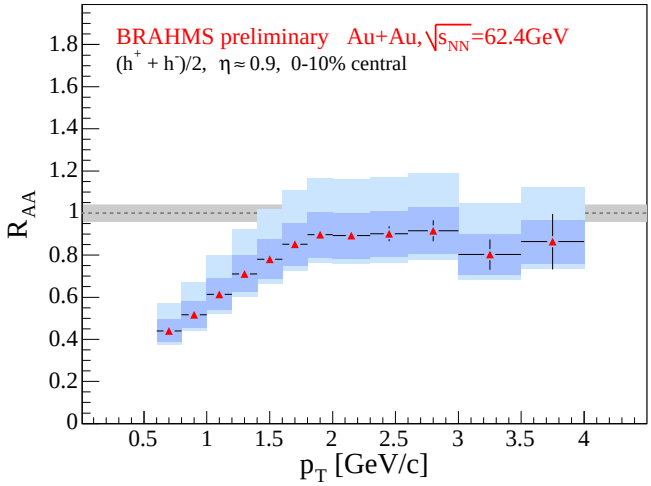

Figure 16. Nuclear modification factor R_{AuAu} measured at $\eta = 0.95$ for $0 - 10\%$ central Au+Au collisions at $\sqrt{s_{nn}} = 62GeV$.[71].

scatterings with the high energy density medium created in the collisions. The quantitative understanding of the observed high p_T suppression, as a function of energy, should be able to determine whether this interaction is at the partonic or hadronic level. This needs to be supplemented by detailed studies of the flavor dependence of the suppression mechanism.

7. The color glass condensate: a model for the initial state of nuclei?

As part as the study of the high p_T suppression in nucleus-nucleus collisions BRAHMS has investigated the rapidity dependence of the nuclear modification factors as a function of rapidity ($\eta = 0, 1, 2.2, 3.2$) in d+Au collisions at $\sqrt{s_{NN}} = 200$ GeV. As discussed in the previous section the measured nuclear modification factors for d+Au are consistent with the absence of high p_T suppression around midrapidity. This has been taken as evidence for the fact that the strong high p_T suppression seen in Au+Au collisions around $y = 0$ is not due to particular conditions in the colliding nuclei (initial state effects) [60,61,60] and [46].

At forward rapidity in d+Au collisions, however, BRAHMS has observed [73] a marked high-p_T suppression starting already at $\eta = 1$ (see Fig. 17 and increasing smoothly in importance with increasing pseudorapidity (up to $\eta = 3.2$). It has been proposed that this effect at forward rapidity [74] is related to the initial conditions of the colliding d and Au nuclei, in particular to the possible existence of the Color Glass Condensate (CGC).

The CGC is a description of the ground state of the nuclei prior to collisions [75]. Nuclei contain a large number of low–x gluons (x is the fraction of the longitudinal momentum carried by the parton) that appears to diverge (grow) with decreasing x. There is however, a characteristic momentum scale, termed the saturation scale, below which the gluon density saturates. This effect sets in when x becomes small and the associated gluon wave length ($\frac{1}{m_p x}$) increases to nuclear dimensions. In such a regime gluons may interact and form a coherent state reminiscent of a condensate. Early indications for the formation of such non-linear QCD systems have been found in lepton-hadron or lepton-

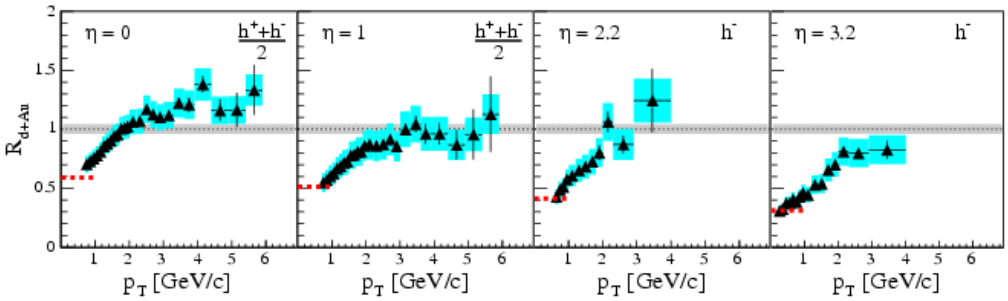

Figure 17. Nuclear modification factors measured in d+Au collisions at pseudorapidities $\eta = 0, 1, 2.2, 3.2$ for central collisions [73].

nucleus collisions at HERA [76] and have been described by the so called "Geometric Scaling" model [77].

The density of gluons $\frac{dN_g}{d(ln(1/x))} \sim \frac{1}{\alpha_s}$ in such a saturated system is high, since α_s, the strong interaction running coupling constant, decreases as the energy increases. The system can therefore be described as a (semi)classical field, and techniques borrowed from field theory can be employed to find the functional form of the parton distributions in the initial state [79].

Saturation in the wave function sets in for gluons with transverse momentum $Q^2 < Q_s^2 = A^{\frac{1}{3}}(\frac{x_0}{x})^{\lambda} \sim A^{\frac{1}{3}}e^{\lambda y}$. A value of $\lambda \sim 0.3$ is estimated from fits to HERA data [78]. The dependence of the saturation scale Q_s on the atomic number of the target and rapidity suggests that saturation effects can be studied with heavy nuclei at large rapidities.

Collisions between heavy ions with energies $E = 100\,\mathrm{AGeV}$ may therefore provide a window to the study of low–x gluon distributions of swiftly moving nuclei. In particular, head-on collisions between deuterons and gold nuclei in which hadrons, produced mostly in gluon-gluon collisions, are detected, close to the beam direction but away from the direction of motion of the gold nuclei, allow the low–x components of the wave function of the gold nuclei to be probed.

The centrality dependence of the nuclear modification factors, provides additional information on the mechanism underlying the observed suppression. Fig. 18 shows the R_{cp} factors, defined as the ratios of the nuclear spectra for central (0-20%) and peripheral (60-80%) collisions (closed points) and for semicentral (30-50%) and peripheral collisions(open points), suitably scaled by the corresponding number of binary collisions, for the four pseudorapidity intervals. There is a substantial change in R_{CP} as a function of η. At $\eta = 0$ the central-to-peripheral collisions ratio is larger than the semicentral-to-peripheral ratios suggesting an increased Cronin type multiple scattering effect in the more violent collisions. In contrast, the more central ratio is the most suppressed at forward rapidities, suggesting a suppression mechanism that scales with the centrality of the collisions.

The observed suppression of yields in d+Au collisions (as compared to p+p) collisions

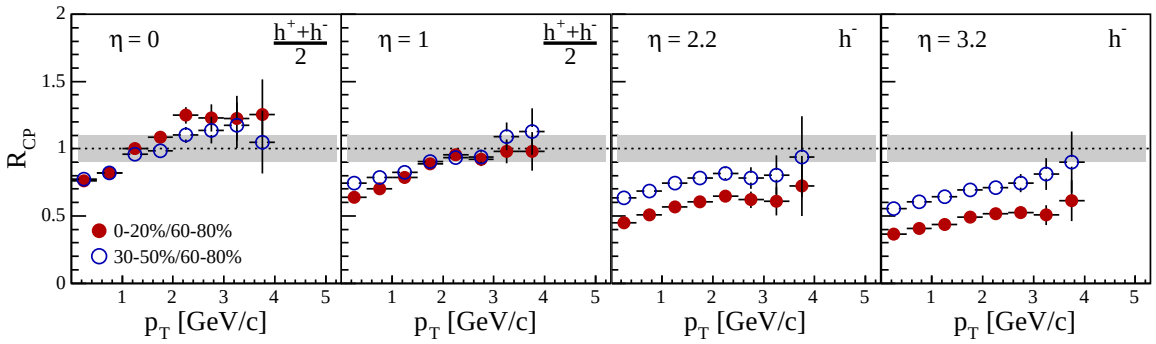

Figure 18. RCP (central to peripheral ratios) as a function of pseudorapidity measured by BRAHMS for d+Au collisions at RHIC top energy [73]

has been qualitatively predicted by various authors [80],[81],[82],[83], within the Color Glass Condensate scenario. Recently, a more quantitative calculation has been carried out [84] which compares well with the data. Other authors [85],[86], have estimated the nuclear modification factors based on a two component model that includes a parametrization of perturbative QCD and string breaking as a mechanism to account for soft coherent particle production using HIJING. HIJING uses the mechanism of gluon shadowing to reduce the number of gluon-gluon collisions and hence the multiplicity of charged particles a lower p_t. HIJING has been shown to give a good description of the overall charged particle multiplicity in d+Au collisions.

The high-p_T-suppression in Au+Au collisions at large rapidites discussed earlier suggests that there may be two competing mechanisms responsible for the observed high-p_T suppression in energetic Au+Au collisions, each active in its particular rapidity window. It has been proposed [7] that the high-p_T suppression observed around midrapidity reflects the presence of an incoherent (high temperature) state of quarks and gluons while the the high-p_T suppression observed at forward rapidities bears evidence of a dense coherent partonic state. Clearly additional analysis of recent high statistics data in Au +Au at high rapidites, as well as firmer theoretical predictions are needed to understand the quantitative importance of gluon saturation effects in energetic nucleus-nucleus collisions.

The suppression of high p_T particles seen at forward rapidities in nucleus-nucleus collisions is a novel and unexpected effect and may be related to a new collective partonic state that describes nuclei at small x.

8. Conclusions and perspectives

The results from the first round of RHIC experiments clearly show that studies of high energy nucleus-nucleus collisions have moved to a qualitatively new physics domain characterized by a high degree of reaction transparency leading to the formation of a near baryon free central region. There is appreciable energy loss of the colliding nuclei, so the conditions for the formation of a very high energy density zone with approximate balance

between matter and antimatter, in an interval of $|y| \lesssim 1.5$ around midrapidity are present.

The indications are that the initial energy density is considerably larger than $5\,GeV/fm^3$, i.e. well above the energy density at which it is difficult to conceive of hadrons as isolated and well defined entities. Analysis within the framework of the statistical model of the relative abundances of many different particles containing the three lightest quark flavors suggest chemical equilibrium at a temperature in the vicinity of $T = 175\,MeV$ and near zero light quark chemical potential. This temperature compares well with the prediction of lattice QCD calculations. The conditions necessary for the formation of a deconfined system of quarks and gluons therefore appear to be present.

However, there are a number of features, early on considered as defining the concept of the QGP, that do not appear to be realized in the current reactions, or at least have not (yet?) been identified in experiment. These are associated with the expectations that a QGP would be characterized by a vanishing interaction betweens quarks and exhibit the features of chiral symmetry restoration and, furthermore, that the system would exhibit a clear phase transition behavior. Likewise, it was originally expected that a QGP phase created in nuclear collisions would be characterized by a long lifetime (up to 100 fm/c) and by the existence of a mixed phase exhibiting large fluctuations of characteristic parameters. In contrast, the body of measurements compared to theory suggest a short lifetime of the system, a large outward pressure and significant interactions most likely at the parton level that result in a seemingly equilibrated system with fluid like properties. Thus the high density phase that is observed, is not identical to the the nearly ideal QGP as it was imagined a decade or two ago.

The central question is, however, as discussed in the introductory chapters, whether the properties of the matter as it is created in todays high energy nucleus–nucleus collisions clearly bears the imprint of a system characterized by quark and gluon degrees of freedom over a range larger that the characteristic dimensions of the nucleon. We know that in nuclei the strong interaction is mediated by a color neutral objects (mesons). Is there experimental evidence that clearly demonstrates interactions based on the exchange of objects with color over distances larger than those of conventional confined objects?

The best candidate for such an effect is clearly the suppression of high transverse momentum particles observed in central Au+Au collisions by the four experiments at RHIC. The remarkably large effect that is observed (a suppression by a factor of 3-5 as compared to peripheral and d+Au collisions) appears readily explainable by radiation losses due to the interaction of high p_T partons with an extended medium (of transverse dimensions considerably larger than nucleon dimensions) consisting of deconfined color charges. Current theoretical investigations, which recently have progressed to attempt first unified descriptions of the reaction evolution, indicate that scenarios based on interactions between hadronic objects cannot reproduce the magnitude of the observed effect.

The interpretation of current data relies heavily on theoretical input and modelling, in particular on the apparent necessity to include partonic degrees of freedom in order to arrive at a consistent description of many of the phenomena observed in the experimental data. Seen from a purely experimental point of view this situation is somewhat unsatisfying, but probably not unexpected, nor avoidable, considering the complexity of the reaction and associated processes.

It is also clear that the unravelling of the physics of the matter state(s) observed at

RHIC has just begun. In spite of the impressive advances that have been made in the last 3 years there are still many issues to be understood in detail, such as the differences in the high-$p_T$suppression of baryons and mesons and the quantitative energy and rapidity dependence of the final and initial state high-$p_T$suppression. Undoubtedly the continued experiments will shed new light on these and many other questions. We should not forget, however, that there are also significant challenges for theory. In the opening chapters of this document we remarked on the requirement that scientific paradigms must be falsifiable. We have yet to see a fully self consistent calculation of the entire reaction evolution at RHIC that in an unambiguous way demonstrates the impossibility of a hadronic description.

In conclusion we find that the body of information obtained by BRAHMS and the other RHIC experiments in conjunction with the available theoretical studies is strongly suggestive of a high density system that cannot be characterized solely by hadronic degrees of freedom but requires a partonic description. Indications are that such a partonic state is not characterized by vanishing interaction of its constituents, but rather by a relatively high degree of coherence such as the one characterizing fluids. At the same time intriguing suggestions of a coherent partonic state at low x in the colliding nuclei has been found.

There is no doubt that the experiments at RHIC have revealed a plethora of new phenomena that for the most part have come as a surprise. In this sense it is clear that the matter that is created at RHIC differs from anything that has been seen before. What name to give it must await our deeper understanding of this matter.

9. Acknowledgements

This work was supported by the Danish Natural Science Research Council, the division of Nuclear Physics of the Office of Science of the U.S. DOE, the Research Council of Norway, the Polish State Committee for Scientific Research and the Romanian Ministry of Research.

REFERENCES

1. J. C. Collins, M. J. Perry, Phys. Rev. Lett. **34**, 1353 (1975); G. Baym, S. A. Chin, Phys. Lett. **B88**, 241 (1976); B. A. Freedman, L. D. McLerran, Phys. Rev. **D16**, 1196 (1977); G. Chapline, Nauenberg, Phys. Rev. **D16**, 450 (1977); E. V. Shuryak, Phys. Lett. **B78**, 150 (1978); O. K. Kalashnikov, V. V. Klimov, Phys. Lett. **B88**, 328 (1979); J. I. Kapusta, Nucl. Phys. **B148**, 461 (1979).
2. H. Satz, Nucl. Phys. **A715**, 3 (2003).
3. CERN press release 2000, http://pressold.web.cern.ch/ PressOld/Releases00/ PR01.00EQuarkGluonMatter.html.
4. M. Adamczyk *et al.*, BRAHMS Collaboration, Nucl. Instr. and Meth. **A499**, 437 (2003).
5. I. G. Bearden *et al.*, BRAHMS Collaboration, Phys. Lett. **B523**, 227 (2001) and Phys. Rev. Lett. **88**, 202301 (2002).
6. BRAHMS exp. homepage: http://www4.rcf.bnl.gov/ brahms/WWW/brahms.html; PHENIX exp. homepage: http://www.phenix.bnl.gov/; PHOBOS exp. homepage: http://www.phobos.bnl.gov/; STAR exp. homepage: http://www.star.bnl.gov/.

7. M. Gyulassy, L. McLerran, nucl-th/0405013.
8. E. V. Shuryak, hep-ph/0405066.
9. P. Jacobs and X. Wang, hep-ph/0405125.
10. C. R. Allton *et al.*, Phys. Rev. **D68**, 014507 (2003), F. Karsch, E. Laermann and A. Peikert, Phys. Lett. **B478**, 447 (2000), F. Karsch, Lect. Notes Phys. **583**, 209 (2002), C. W. Bernard *et al.*, Phys. Rev. **D55**, 6861 (1997), S. Gupta, Pramana **61**, 877 (2003), Z. Fodor and S. D. Katz, hep-lat/0402006, F. Csikor *et al.*, hep-lat/0401022.
11. F. Videbæk and O. Hansen, Phys. Rev. **C52**, 26 (1995).
12. W. Busza and A. S. Goldhaber, Phys. Lett. **B139**, 235 (1984).
13. W.Busza and R.Ledoux, Ann.Rev.Nucl.Science **38** 150 (1988).
14. B. B. Back *et al.*, Phys. Rev. Lett. **86**, 1970 (2001).
15. L. Ahle *et al.*, Phys. Rev. **C60**, 064901 (1999).
16. J. Barette *et al.*, Phys. Rev. **C62**, 024901 (2000).
17. H. Appelshauser *et al.*, Phys. Rev. Lett. **82** 2471 (1999).
18. BRAHMS collaboration, Nucl. Phys.**A715**, 171c (2003) and *ibid* p. 482c, BRAHMS collaboration nucl-ex/0312023, and P. Christiansen, Ph. D. thesis, Univ. Copenhagen, June 2003., nucl-ex/0312023.
19. J. D. Bjorken, Phys. Rev. D**27**, 140 (1983).
20. J. W. Harris and B. Müller, Ann. Rev. Nucl. Part. Sci. **46**, 71 (1996).
21. K. J. Eskola and Xin-Nian Wang, Phys. Rev. **D49**, 1284 (1994).
22. F. Karsch, Nucl. Phys. **A698**, 199 (2002).
23. M. Gyulassy and T. Matsui, Phys. Rev. **D29**, 419 (1984).
24. R. Stock, Phys. Lett. **B456**, 277 (1999).
25. D. Ouerdane, Ph.D. thesis, Univ. Copenhagen, August 2003, I. G. Bearden *et al.*, BRAHMS Collaboration, nucl-ex/0403050 and references therein.
26. I. G. Bearden *et al.*, BRAHMS Collaboration, Phys. Rev. Lett. **90**, 102301 (2003).
27. P. Koch *et al.*, Phys. Rep. **142** (1986) 167.
28. J. Cleymans *et al.* Z. Phys. **C57** (1993) 135.
29. J. Cleymans *et al.* Nucl. Phys. **A566** (1994) 391.
30. P. Braun-Munzinger *et al.*, Phys. Lett. B **518**, 41 (2001).
31. F. Becattini *et al.*, Phys. Rev. C**64**, 024901 (2001) and private communication.
32. J. Cleymans, J. Phys. **G28**, 1576 (2002).
33. S. S. Adler *et al.*, PHENIX collaboration, Phys. Rev. Lett. **91**, 182301 (2003).
34. S. S. Adler *et al.*, PHENIX collaboration, Phys. Rev. Lett. **89**, 212301 (2002).
35. B. B. Back *et al.*, PHOBOS collaboration, Phys. Rev. Lett. **89**, 222301 (2002).
36. C. Adler *et al.*, STAR collaboration, Phys. Rev. **C66**, 034904 (2002).
37. C. Adler *et al.*, STAR collaboration, Phys. Rev. Lett. **87**, 182301 (2001).
38. C. Adler *et al.*, STAR collaboration, Phys. Rev. Lett. **86**, 402 (2001).
39. P. F. Kolb, J. Sollfrank, U. Heinz, Phys. Lett. **B459**, 667 (1999).
40. P. Huovinen, P. F. Kolb, U. Heinz, P.V. Ruuskanen, S. A. Voloshin, Phys. Lett. **B503**, 58 (2001).
41. D. Molnar, S. A. Voloshin, Phys. Rev. Lett. **91**, 092301 (2003).
42. D. Teaney, J. Lauret, E. V. Shuryak, Phys. Rev. Lett. **86**, 4783 (2001).
43. H. Sorge, Phys. Rev. Lett. **82**, 2048 (1999).
44. H. Heiselberg and A. M. Levy, Phys. Rev. **C59**, 2716 (1999).

45. P. F. Kolb, P. Huovinen, U. Heinz, H. Heiselberg, Phys. Lett. **B500**, 232 (2001).
46. I. Arsene *et al.*, BRAHMS collaboration, Phys. Rev. Lett **91**, 072305 (2003).
47. J. Adams *et al.*, Phys. Rev. Lett. **91**, 172302 (2003).
48. S. S. Adler *et al.*, Phys. Rev. **C69**, 034910 (2004).
49. B. Back *et al.*, Phys. Lett. **B578**, 297 (2004).
50. R. Baier *et al.*, Phys. Lett. **B345**, 277 (1995).
51. M. Gyulassy and M. Plümer, Phys. Lett.**B243**, 432 (1990).
52. X. N. Wang and M. Gyulassy, Phys. Rev. Lett. **68**, 1480(1992).
53. J. D. Bjorken, Report No. Fermilab-Pub-82/59-THY (1982).
54. R. Baier, D. Schiff, B.G. and Zakharov, Ann. Rev. Nucl. Part. Sci. **50**, 37 (2000).
55. C. Adler *et al.*, Phys. Rev. Lett. **90**, 082302 (2003).
56. C. E. Jørgensen *et al.*, BRAHMS collaboration, Nucl. Phys. A715 741c (2003).
57. J. W. Cronin *et al.*, Phys. Rev. **D11** 3105 (1975).
58. A. Accardi, hep-ph/0212148.
59. D. Kharzeev, E. Levin, L. McLerran, Phys. Lett. **B561**, 93 (2003) and references therein.
60. J. Adams *et al.*, Phys. Rev. Lett. **91**, 072304 (2003).
61. B. B. Back *et al.* nucl-ex/0302015 and Phys. Rev. Lett. **91**, 072302 (2003).
62. S. S. Adler *et al.*, Phys. Rev. Lett. **91**, 072303 (2003).
63. M. M. Aggarwal *et al.*, Eur. Phys. J. **C18**, 651 (2001).
64. G. Agakishiev *et al.*, hep-ex/0003012.
65. Z. Yin, BRAHMS Collaboration, to be published in J. Phys. **G**.
66. B. Alper *et al.*, Nucl. Phys. **B100**, 237 (1975).
67. P. Abreu *et al.*, Eur. Phys. J. **C17**, 207 (2000).
68. R. C. Hwa and C. B. Yang, Phys. Rev. **C67**, 034902 (2003).
69. R. J. Fries *et al.*, Phys. Rev. **C68**, 044902 (2003).
70. V. Greco, C. M. Ko and P. Levai, Phys. Rev. Lett. **90**, 202302 (2003).
71. BRAHMS Collaboration, in preparation; C.Ekman, Ph.D. Thesis, University of Copenhagen, 2004.
72. B. Back *et al.*, submitted to Phys. Rev. Lett. (nucl-ex/0405003).
73. I. Arsene *et al.*, BRAHMS collaboration, Submitted to Phys.Rev.Lett., nucl-ex/0403005
74. D. Kharzeev, E. Levin and L. McLerran Phys. Lett. **B561** 93-101 (2003).
75. L. V. Gribov, E. M. Levin and M. G. Ryskin, Phys. Rept. **100**, 1 (1983), A. H. Mueller and Jian-wei Qiu, Nucl. Phys. **B268**, 427 (1986), L.N. Lipatov, Sov. J. Nucl. Phys. **23** (1976), 338, E.A. Kuraev, L.N. Lipatov and V.S. Fadin, Sov. Phys. JETP 45 (1977), 199G Ya.Ya. Balitsky and L.N. Lipatov, Sov. J. Nucl. Phys. **28**, 822 (1978), L. D. McLerran and R. Venugopalan, Phys. Rev. **D49**, 2233(1994) 3352 (1994); D50, 2225 (1994), E. Iancu, A. Leonidov and L. D. McLerran, Nucl. Phys. **A692**, 583 (2001), E. Iancu and L. McLerran, Phys.Lett. **B510**, 145 (2001).
76. J. Breitweg *et al.* Eur. Phys. J. C7 609-630, (1999); ZEUS Collaboration, J. Breitweg *et al.*, Phys. Lett. **B487** (2000) 53; ZEUS Collaboration, S. Chekanov *et al.*, Eur. Phys.J. **C21** (2001) 443; H1 Collaboration, C. Adloff *et al.*, Eur. Phys. J. **C21** (2001) 33.
77. A. M. Staśto, K. Golec-Biernat, and J. Kwieciński Phys. Rev. Lett. 86 596-599 (2001).

78. J. Breitweg *et. al.*, Phys. Lett. **B407**, 432 (1997).
79. L. McLerran and R. Venugopalan, Phys. Rev. **D49**, 2233(1994); Phys. Rev. **D59**, 094002 (1999); E. Iancu, A. Leonidov and L. D. McLerran, Nucl. Phys. **A692**, 583 (2001), and references therein.
80. A. Dumitru and J. Jalilian-Marian, Phys. Lett. B **547**, 15 (2002)
81. J. Jalilian-Marian, Y. Nara and R. Venugopalan, Phys. Lett. B **577**, 54 (2003); A. Dumitru and J. Jalilian-Marian Phys. Rev. Lett. 89 022301 (2002).
82. R. Baier *et al.* Phys. Rev. D68, 054009, (2003); J. Albacete, *et. al.*, hep-ph/0307179.
83. D. Kharzeev, Y. V. Kovchegov and K. Tuchin Phys. Rev. D68, 094013, (2003); D. Kharzeev, E. Levin and L. McLerran, Phys. Lett. B **561**, 93 (2003).
84. D. Kharzeev, Y. V. Kovchegov, and K. Tuchin, hep-ph/0405045.
85. I. Vitev, Phys. Lett. **B562**, 36 (2003)
86. Xin-Nian Wang, Phys. Lett. **B565**, 116-122, (2003).